RMetS
Royal Meteorological Society

Tidal effects on stratospheric temperature series derived from successive advanced microwave sounding units

P. Keckhut,[a]* B. M. Funatsu,[a,b,c] C. Claud[c] and A. Hauchecorne[a]

[a]*Laboratoire Atmosphères, Milieux, Observations Spatiales, CNRS UMR 8190, Université de Versailles Saint-Quentin, Guyancourt, France*

[b]*LETG-Rennes COSTEL, CNRS UMR 6554, Université Rennes 2, Rennes, France*

[c]*Laboratoire de Météorologie Dynamique, CNRS UMR 8539, IPSL, Ecole Polytechnique, Palaiseau, France*

*Correspondence to: P. Keckhut, Laboratoire Atmosphères, Milieux, Observations Spatiales, CNRS UMR 8190, Université de Versailles Saint-Quentin, Guyancourt, France. E-mail: philippe.keckhut@latmos.ipsl.fr

Stratospheric temperature series derived from the Advanced Microwave Sounding Unit (AMSU) on board successive NOAA satellites reveal, during periods of overlap, some bias and drifts. Part of the reason for these discrepancies could be atmospheric tides as the orbits of these satellites drifted, inducing large changes in the actual times of measurement. NOAA 15 and 16, which exhibit a long period of overlap, allow deriving diurnal tides that can correct such temperature drifts. The characteristics of the derived diurnal tides during summer periods is in good agreement with those calculated with the Global Scale Wave Model, indicating that most of the observed drifts are likely due to the atmospheric tides. Cooling can be biased by a factor of 2, if times of measurement are not considered. When diurnal tides are considered, trends derived from temperature lidar series are in good agreement with AMSU series. Future adjustments of temperature time series based on successive AMSU instruments will require considering corrections associated with the local times of measurement.

Key Words: satellite; temperature; stratosphere; tides

Received 7 October 2013; Revised 13 March 2014; Accepted 19 March 2014; Published online in Wiley Online Library 27 May 2014

1. Introduction

According to observations, the stratosphere has cooled over the last decades (Randel *et al.*, 2009). Chemistry climate model intercomparisons (Shine *et al.*, 2003; Austin *et al.*, 2009) indicate that the upper stratospheric trends were driven by ozone depletion and the increase in carbon dioxide, while feedback contributions including increases in stratospheric water vapour (Solomon *et al.*, 2010), cloud occurrence (Wylie *et al.*, 2005) and dynamical changes (Angot *et al.*, 2012) are not well quantified. The agreement between models and observed temperatures trends showed improvement as of the last assessment (Austin *et al.*, 2009); models have introduced interactive ozone chemistry and included a slightly colder climatology, yet large differences both between models and between models and observations still persist.

Trend analyses are standard diagnostics for evaluating stratospheric climate model performance (Powell *et al.*, 2013). Observations of stratospheric temperature trends have been regularly assessed as part of the World Meteorological Organisation/United Nations Environment Programme (WMO/UNEP) Scientific Assessments on Ozone Depletion (WMO, 2007) and the Intergovernmental Panel on Climate Change (IPCC) assessment of climate changes (IPCC, 2007). Several different research experiments providing atmospheric temperature have operated on board satellites. However, because their objectives, lifetime and the techniques involved are so different, the time continuity over more than a decade has been difficult to keep. Estimates of global past temperature trends in the middle and upper stratosphere rely primarily on a single dataset derived from the successive operational Stratospheric Sounding Unit (SSU) instruments. The derived series exhibit substantial uncertainties including change of the vertical weighting functions due to atmospheric CO_2 changes (Shine *et al.*, 2008), radiometric drifts and atmospheric tides (Nash and Forrester, 1986). Essentially, there are two SSU datasets available for the research community: the first was produced by Nash and colleagues (Nash and Brownscombe, 1982; Nash and Forrester, 1986; Nash, 1988; Nash and Edge, 1989), and extensively used for several years as it was the only available SSU analysis (even though details of data processing are largely unknown); and a second, recently released SSU analysis from the National Oceanic and Atmospheric Administration (NOAA) Center for Satellite Applications and Research (Wang *et al.*, 2012). The latter takes into account the aforementioned uncertainties and corrects for the limb effect due to varying angles-of-view of

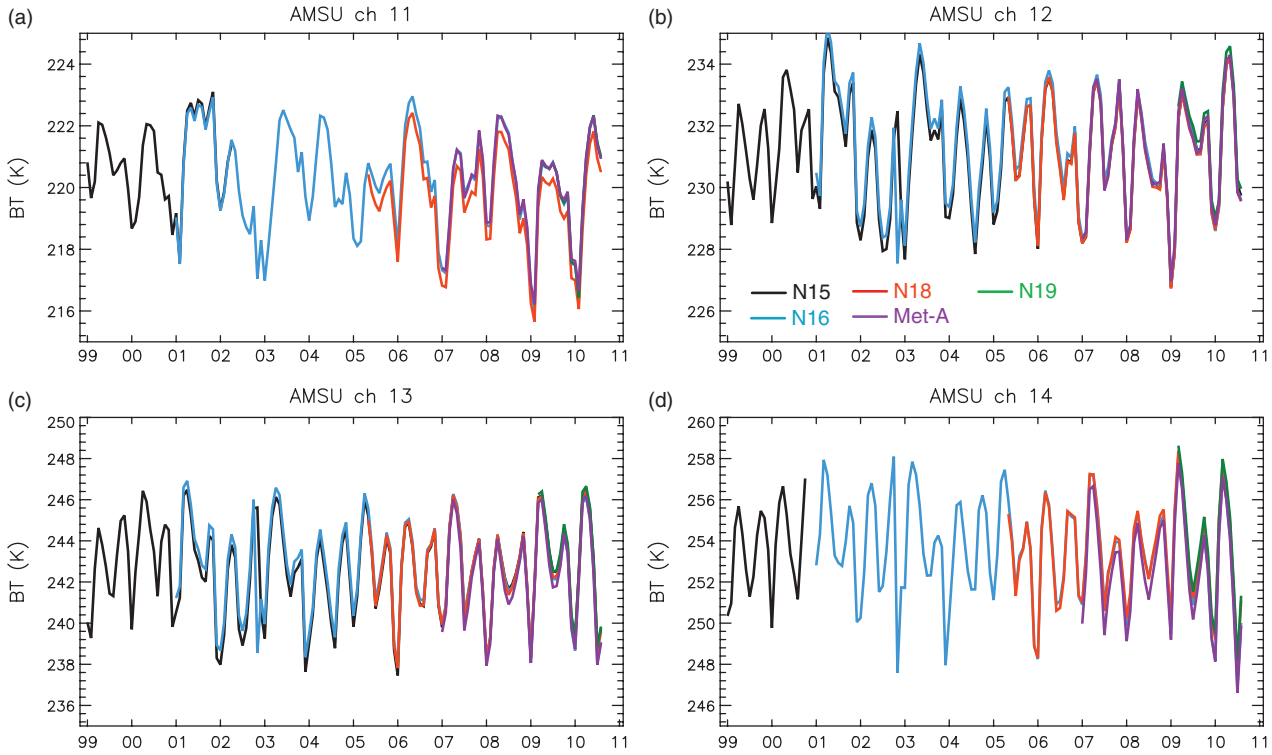

Figure 1. Zonal mean temperature series averaged on the 10°N to 10°S latitude band for 1999–2010, given by the successive AMSU for the four stratospheric levels 11, 12, 13 and 14 on respectively panels (a), (b), (c) and (d). AMSU data obtained on NOAA-15 are represented in black, NOAA-16 in blue, NOAA-17 in red, NOAA-18 in green and Metop-A in purple.

the SSU instrument; all procedure is extensively documented in Wang *et al.* (2012), and the dataset has been cross-evaluated with lidar, Global Positioning System (GPS) radio occultation and Microwave Limb Sounder observations (Wang and Zou, 2013). Trends derived from these two datasets lead to different trend estimates (Thompson *et al.*, 2012; Wang *et al.*, 2012) in the middle and upper stratosphere. For example, the old SSU series for the lowest stratospheric channel show that there has been no cooling in the global mean since the early 1990s and cooling is not obvious between the two largest volcanic eruptions (El Chichón in 1982 and Pinatubo in 1991). However, trends derived from the new NOAA SSU dataset show strong cooling in the mid-stratosphere for the period 1979–2006, i.e. including the period after 1990 (Wang *et al.*, 2012). These studies show that adjustments between series are critical to analyse temperature trends. The continuation of temperature monitoring in the mid upper-stratosphere from space relies now on the successive Advanced Microwave Sounding Unit (AMSU) instruments that replace SSU, providing similar altitude range with however sharper vertical weighting functions. The adjustment of the successive AMSUs in order to detect reliable temperature changes over a period longer than the lifetime of a single instrument represents a formidable challenge. The inter-calibration of the instruments simultaneously in space has been rendered difficult because of different times of measurement, and even more complex due to the orbit drifts (e.g. Zou and Wang, 2011).

The purpose of this study is to estimate instrument calibration differences by taking into account tidal effects for the purpose of correcting series from these effects. The AMSU measurements are described in section 2, while section 3 describes tidal corrections and the remaining calibration difference. Impact on trends is discussed in section 4. Finally, discussions about the methodology and the impact on a future strategy are included in section 5.

2. AMSU description

This study focuses on the stratosphere temperature monitoring by using the temperature data from AMSU-A. This spectrometer is a cross-scanning microwave instrument that is composed of 15 channels between 50 and 58 GHz in the oxygen band, allowing the observation of the temperature structure of the atmosphere from the surface to around 50 km. More specifically, six channels (from 9 to 14) sound the stratosphere with vertical weighting functions with half-width of around 10 km (Karbou *et al.*, 2005). The weighting functions for these channels are centred approximately at 18, 20, 25, 30, 35 and 40 km, respectively. The AMSU instrument has been collecting observations on board several successive NOAA polar-orbiting satellites (NOAA-15 through to -19, starting in 1998, 2000, 2002, 2005 and 2009 respectively), National Aeronautics and Space Administration Earth Observing System (NASA EOS-Aqua) satellite (since May 2002), and Metop (Metop-A in 2006 and Metop-B launched in 2012). In principle, it consists of quite homogeneous data as the same instrument is used; however, the same instrument on different platforms may yield slightly different measurements when overlooking the same position at the same time; this issue will be discussed further on. Given a 'target' area, two overpasses per day are generally available, thus zonal means using both ascending and descending passes are calculated for several latitudinal bands ranging from 80°S to 80°N. Only measurements of the near-nadir field-of-view tracking position are taken to avoid limb effects that affect the effective centre of the weighting function (Goldberg *et al.*, 2001). The superposition of temperature measurements from the successive AMSU instruments shows consistent monthly-mean zonal-mean temperature series with similar interannual variability and agreements better than 1 K (Figure 1). Such differences are small; however, they induce uncertainties on trend calculations. Fortunately, the AMSU series exhibit several overlapping periods. When temperatures obtained for the same period from different AMSU instruments are compared, systematic differences can be noted (Figure 2(a) for 10°N to 10°S latitude band). At some levels (channels 12 and 13, Figure 2(c) and (d), respectively) and for some coupled AMSU, drifts can also be observed with the largest amplitudes for data series corresponding to the upper altitude levels. NOAA-15 and NOAA-16 AMSU-A, which provide the longest period of operation and a long overlapping period, show obvious drifts for channels 12 and 13 (AMSU channel 14 on NOAA-15 failed in October 2000). Such drifts are assumed

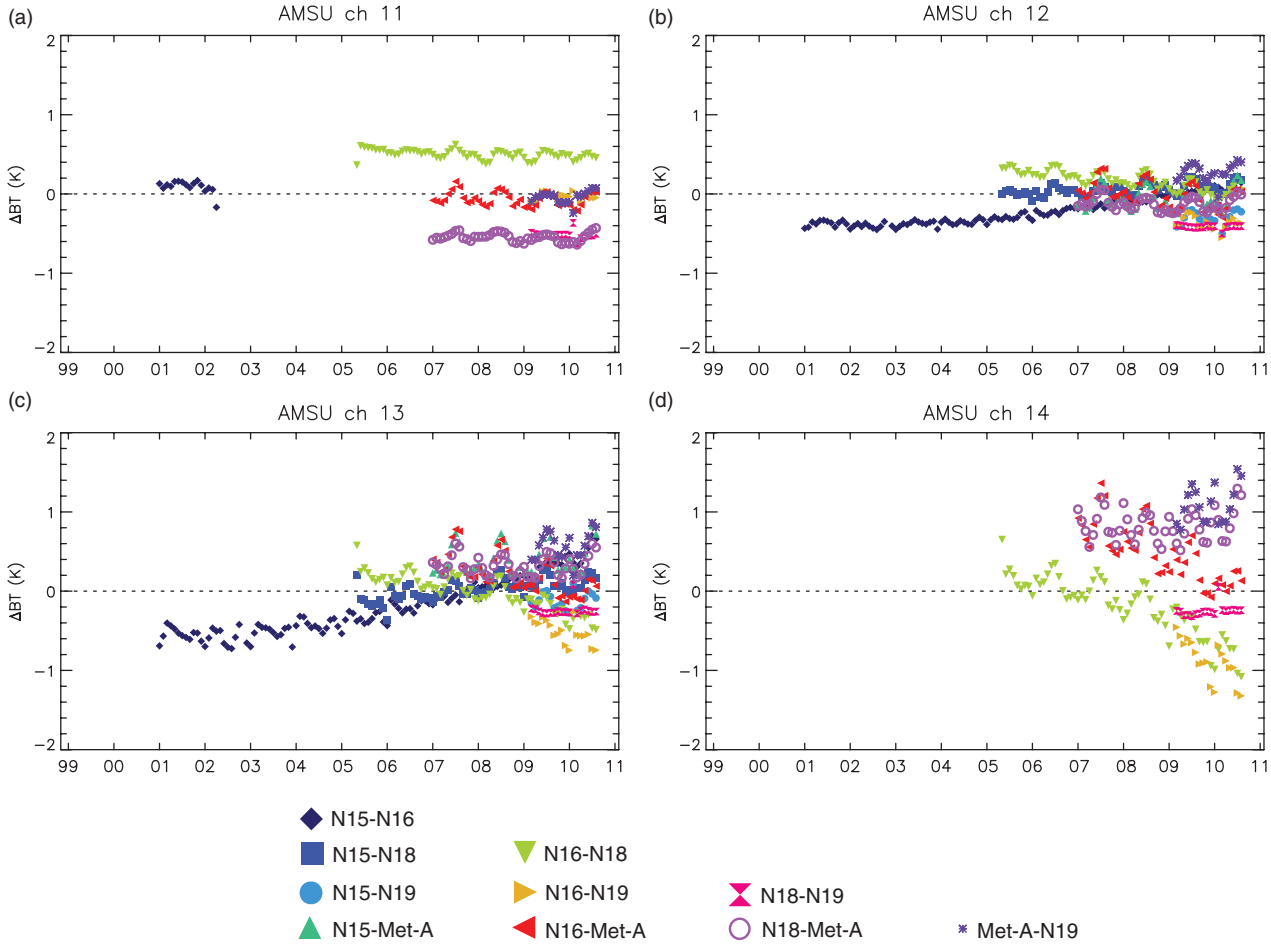

Figure 2. (a)–(d) Monthly mean brightness temperature differences from pairs of different platforms (N15 is NOAA-15 etc.) for AMSU channels 11, 12, 13 and 14 for the latitudinal band 10°S to 10°N, years 2001–2010.

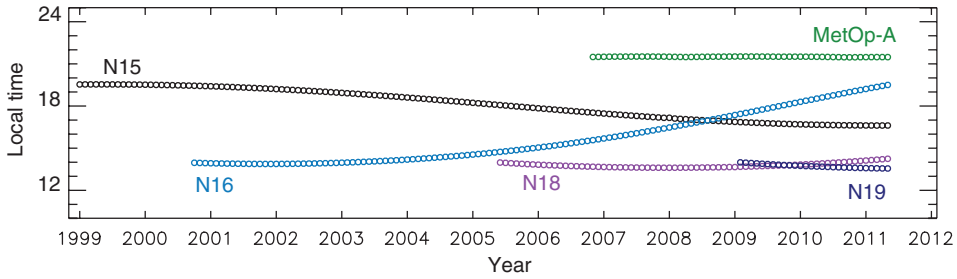

Figure 3. Equatorial crossing time (local) of temperature measurements for the AMSU instruments on board the different satellites for ascending orbits.

to be associated with atmospheric tides since orbit drifts induce changes of the times of measurement (Figure 3). This has already been reported for the Microwave Sounding Unit (MSU) series on successive NOAA satellites (Mears *et al.*, 2002) with mean effects in the troposphere of a few tenths of a degree, with however large regional effects related to orography and convection.

Recently, Zou and Wang (2011) performed AMSU inter-calibration, adjusting all AMSU measurements with respect to those collected by that on NOAA-15 using the Simultaneous Nadir Overpass (SNO) method (Cao *et al.*, 2004). The new, inter-calibrated data, named 'AMSU IMICA' (Integrated Microwave Inter-Calibration Approach) is currently available (as of January 2014) through NOAA's National Climatic Record Center Climate Data Record Program site at http://www.ncdc.noaa.gov/cdr/operationalcdrs.html. This dataset takes into account and corrects biases found in the pre-launch AMSU observations, including: relatively stable inter-satellite biases between most satellite pairs, instrumental drifts, sun-heating-induced instrument temperature variability in radiances, and scene temperature dependency in biases due to inaccurate calibration nonlinearity. NOAA also made available the full operational AMSU data along with data with limb-correction following Goldberg *et al.* (2001). When using only near-nadir data to construct the time series, the range of temperature differences between NOAA-15 and NOAA-16 from both IMICA and operational AMSU are basically unchanged (Figure 4), whereas using all fields-of-view to calculate monthly means yields temperature differences smaller for IMICA than for limb-corrected AMSU, within however the same order of magnitude and same sign of slope (not shown). This indicates that the diurnal cycle component present in the data is not completely removed in the IMICA data series, as the SNO method uses matched pairs that are geographically and temporally close, and thus free from the effects of the diurnal drift.

3. Quantification of tidal effects

AMSU data from NOAA-15 and NOAA-16 provide a good opportunity to investigate the source of the differences and the possibility to correct them as both provide the longest period of operation and a long overlapping period since January 2001. Channel 13 was chosen, as the temperature differences are

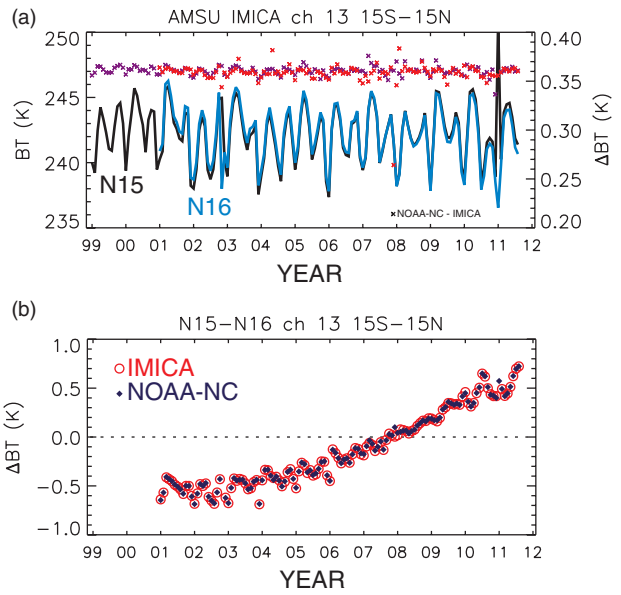

Figure 4. (a) AMSU IMICA monthly mean temperature series for the equatorial region (15°S to 15°N), 1999–2011, given by instruments on board NOAA-15 (black) and NOAA-16 (blue). Differences between IMICA and operational data are also shown (crosses). Notice that only near-nadir data were used to construct the monthly mean time series. (b) Temperature differences (NOAA-15 minus NOAA-16) retrieved from AMSU operational (black) and IMICA (red) analyses from AMSU channel 13 are reported.

Table 1. (a) Tidal amplitude and (b) phase for different latitude bands derived from two AMSU instruments (NOAA-15, NOAA-16) measuring in the same period on different orbits, as well as (e) systematic bias. (c),(d) GSWM-00 tidal amplitude and phase estimates (upgrade from Hagan *et al.*, 1999).

Latitude domain	(a) N15, N16 AMSU tidal amplitude (K)	(b) N15, N16 AMSU tidal phase (h)	(c) GSWM tidal amplitude (K)	(d) GSWM tidal phase (h)	(e) Bias N16-N15 (K)
60–80°N	0.29	14.1	0.26	13.5	−0.052
45–60°N	0.21	17.3	0.28	20.0	−0.076
30–45°N	0.20	17.8	0.31	21.7	−0.088
15–30°N	0.32	21.4	0.30	20.1	−0.089
15°S–15°N	0.70	22.6	0.73	16.0	−0.084
15–30°S	0.49	22.4	0.28	19.2	−0.067
30–45°S	0.60	17.7	0.32	22.2	−0.070
45–60°S	0.21	17.1	0.23	18.6	−0.074
60–80°S	0.60	20.8	0.27	11.2	−0.155
All	–	–	–	–	−0.084

obtained for the longest period while both instruments on NOAA 15 and 16 are in operation simultaneously over a long period (decade). Drifts evolve in the opposite direction, and in mid-2008 both satellites presented measurements at nearly the same time of day. Data obtained during this specific period can be used to calculate temperature differences that can be associated with instrumental differences, as temperature anomalies induced by atmospheric tides are similar. Small but robust values around 0.08 K are derived (Table 1), with AMSU temperature on NOAA-15 being slightly warmer than temperature from NOAA-16. These estimates were obtained by first constructing monthly mean temperatures for nine latitude bands (80 to 60°N and S, 60 to 45°N and S, 45 to 30°N and S, 30 to 15°N and S, and 15°S to 15°N). Then, the mean temperature differences were calculated for each latitude band (Table 1). Except for the southern high latitudes, where the variability is large, the temperature differences are similar. Such results are expected since the same instrument is used for measurements in all latitude bands. The temperature evolution reveals monotonic drifts as a function of time (Figure 5) with varying amplitude according to the latitude bands. This systematic difference is in good agreement with that of about −0.08 K inferred by the bias adjustment scheme used in the ERA-Interim data assimilation system (Simmons *et al.*, 2014), which does not show strong sensitivity to orbital drift. In the summer stratosphere, the main tidal mode is a 24 h oscillation (Keckhut *et al.*, 1996). The diurnal tides exhibit a seasonal cycle with amplitudes that increase with latitude, and the amplitude of the semi-diurnal mode increases too (Keckhut *et al.*, 1996), leading to a tidal behaviour that is more complex at high latitudes. This simple tidal model explains the appearance of an annual oscillation in the temperature difference between AMSU instruments. Here, only diurnal tide is considered and only summer data for each respective hemisphere (June, July, August and December, January, February respectively for Northern and Southern Hemispheres) are used to derive a tidal correction. Temperature anomalies at a given time t, and at an altitude z induced by tides $tide(t,z)$ can be expressed as:

$$tide(t,z) = a(z)\cdot\cos\{(2\pi t/24) - \phi(z)\}, \quad (1)$$

with $a(z)$ and $\phi(z)$ being respectively the amplitude of the tide and phase (time of the maximum). It can be also expressed as:

$$tide(t,z) = a_1(z)\cdot\sin\{2\pi t\} + a_2(z)\cos\{2\pi t\}, \quad (2)$$

with $a_1(z)$ and $a_2(z)$ being the amplitude of two out-of-phase functions.

The amplitude and phase of the tides can be calculated from $a_1(z)$ and $a_2(z)$:

$$a(z) = \sqrt{a_1^2(z) + a_2^2(z)} \text{ and } \phi(z) = \arctan\left(\frac{a_1(z)}{a_2(z)}\right). \quad (3)$$

While the large-scale temperature change over the diurnal scale is negligible (that is the case during summer months), the difference between two collocated temperature measurements obtained at different times t_1 and t_2 can be deduced from Eq. (2) and expressed as follows:

$$\Delta T(z) = a_1(z)\cdot\sin\{2\pi(t_2 - t_1)\} + a_2(z)\cdot\cos\{2\pi(t_2 - t_1)\}. \quad (4)$$

Since the time difference is known (Figure 3), a least-square fit was applied on the difference temperature series in summer (except for the equatorial band where all the data are considered) and parameters a_1 and a_2 were calculated for each altitude level z; amplitude and phase were calculated using Eq. (3) and reported in Table 1.

In addition to a drift, a seasonal cycle is clearly visible that is due to the seasonal evolution of the tidal amplitude. Phase values are similar to previous estimates with lidar (Keckhut *et al.*, 1996), while amplitudes are smaller probably because of vertical smoothing caused by the large vertical weighting function of AMSU. The tidal characteristics derived from both instruments have been compared with the Global Scale Wave Model (GSWM: Hagan *et al.*, 1999) developed by Hagan to study tides (1998) which provided zonal estimates. There is an even better agreement with the values derived here with AMSU series than with the lidar, maybe because the vertical resolutions are similar. The amplitudes show differences smaller than 10% in most of the latitude bands except for the Southern Hemisphere where differences increase up to 50%. As the amplitude estimates depend on vertical resolution, the phase is a more valuable parameter to qualify the agreement.

Phases agree within 2–3 h except for high southern latitudes where large differences are observed. However, we note that these values agree with recent lidar observations performed at Dumont D'Urville (David *et al.*, 2012). A detailed view of the tide behaviour reveals that there is a strong gradient of the phase from 1000 to 2000 h (solar time) around the peak of the weighting function of channel 13 (for more detail, visit http://www.hao.ucar.edu/modeling/gswm/gswm.html; for the tidal generator associated with a more recent version of

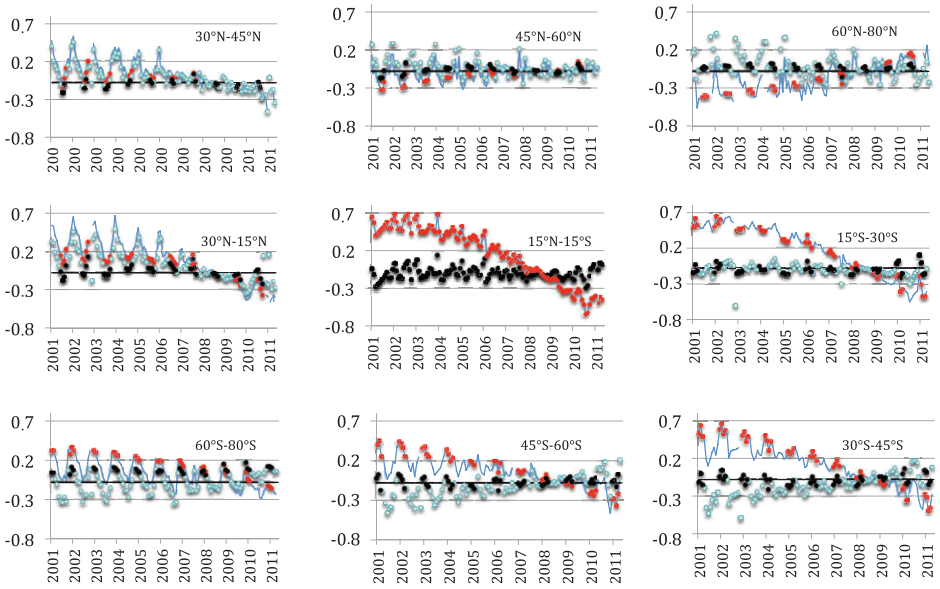

Figure 5. Channel 13 temperature differences between AMSU NOAA 16 and 15 (N16 – N15) for nine latitude bands from pole to pole (blue lines). Differences of raw summer data (for each respective hemisphere) are indicated in red dotted marks except for the equatorial band where *all* the differences are indicated with red dotted marks. Tide-corrected summer data are plotted with black marks while the other seasons, corrected with the summer tidal model, are indicated by light green dots.

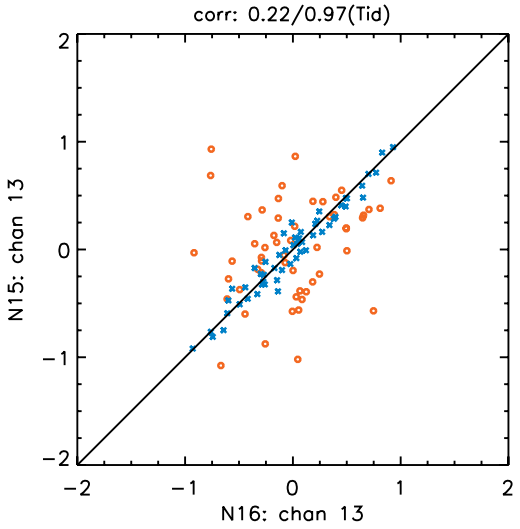

Figure 6. Comparisons between raw AMSU NOAA-15 and NOAA-16 channel 13 temperature data (orange) and N15 and N16 after tidal corrections (blue), for summer months only in the 30–45°N latitude band.

the GSWM model: Zhang *et al.*, 2010). When the whole series are corrected with the 'summer' estimates, drifts are reduced while a seasonal cycle remains. This model applied to summer (for each corresponding hemisphere) data for AMSU on both NOAA-15 and NOAA-16 satellites show that the differences can be reduced (Figure 6). Once the tidal correction is applied on data series at mid to high latitudes long-term drifts are removed (Figure 5), but differences still exhibit a seasonal oscillation associated with the tidal seasonal cycle and the semi-diurnal mode. This analysis can be extended to other channels. However, channel 12, with weighting function peaking at a lower altitude, is expected to be less influenced by tidal effects because tidal amplitudes are smaller. Channel 14 also exhibits large drifts (Figure 2) but the overlapping period is relatively short because channel 14 on NOAA-15 failed by the end of October 2000, and AMSU on NOAA-17 failed in 2003; thus the longest overlapping series are those of NOAA-16 and NOAA-18 from mid-2005.

4. Effects on trend estimates

When both temperature series (NOAA 15 and 16) are compared, a good correlation is observed while some differences due to tides are superimposed. When this effect is corrected with the derived tidal model (Table 1), the correlation increases considerably (Figure 6) and a regression coefficient is derived with a slope of 1.

AMSU series have been also compared with temperature lidar series. Few sites within the international Network for the Detection of Atmospheric Composition Change (NDACC) provide decadal series (Keckhut *et al.*, 2004, 2011). The lidar operating on Table Mountain, California, is the only NDACC site that can provide a sufficiently large time sampling during summer months to correctly trap the interannual variability (Leblanc *et al.*, 1998).

AMSU summer data are selected to compare raw and tidal corrected temperature data with those derived by the Table Mountain Facility (TMF) lidar. The corresponding altitude between lidar and AMSU channel 13 has been determined following the same method as that developed by Funatsu *et al.* (2008). Raw AMSU temperature series show differences on tendencies (around 15%) with lidar time evolution for both instruments on board NOAA 15 and 16 (Figure 7). The NOAA-15 temperature dataset shows reduced tendencies (-0.5 ± 0.5 K decade^{-1}) and NOAA-16 shows larger tendencies (-0.9 ± 0.5 K decade^{-1}). The tendency difference for correct/non-correct NOAA series is nearly significant (95%) while uncertainties are all provided for the 2σ interval. When NOAA temperature series are corrected for atmospheric tides, the tendencies converge to a similar median value (-0.6 ± 0.4 K decade^{-1}) close to the lidar estimate (-0.7 ± 0.8 K decade^{-1}). Wang and Zou (2014) also found a trend of -0.66 K decade^{-1} for channel 13, based on IMICA data records for the period 1998–2011.

The above tendencies are estimated using a straight line fitting the NOAA-15 temperature series with a least-square method and show for the tropical band (where tides exhibit larger amplitudes) a cooling of 0.35 K decade^{-1} (Figure 8). When the tidal correction is applied, the cooling trend is larger and increases to 0.85 K decade^{-1}. This correction is quite important since the trend enhancement is more than twice the original estimates. This present trend estimate, fully independent of any atmospheric models, is in better agreement with trends calculated with both ERA-Interim analyses and CMIP5 models that are not biased by tidal effects (Simmons *et al.*, 2014).

5. Discussion and conclusions

Drifts of the orbits for the instruments in space are a key issue for stratospheric temperature analysis due to atmospheric tides.

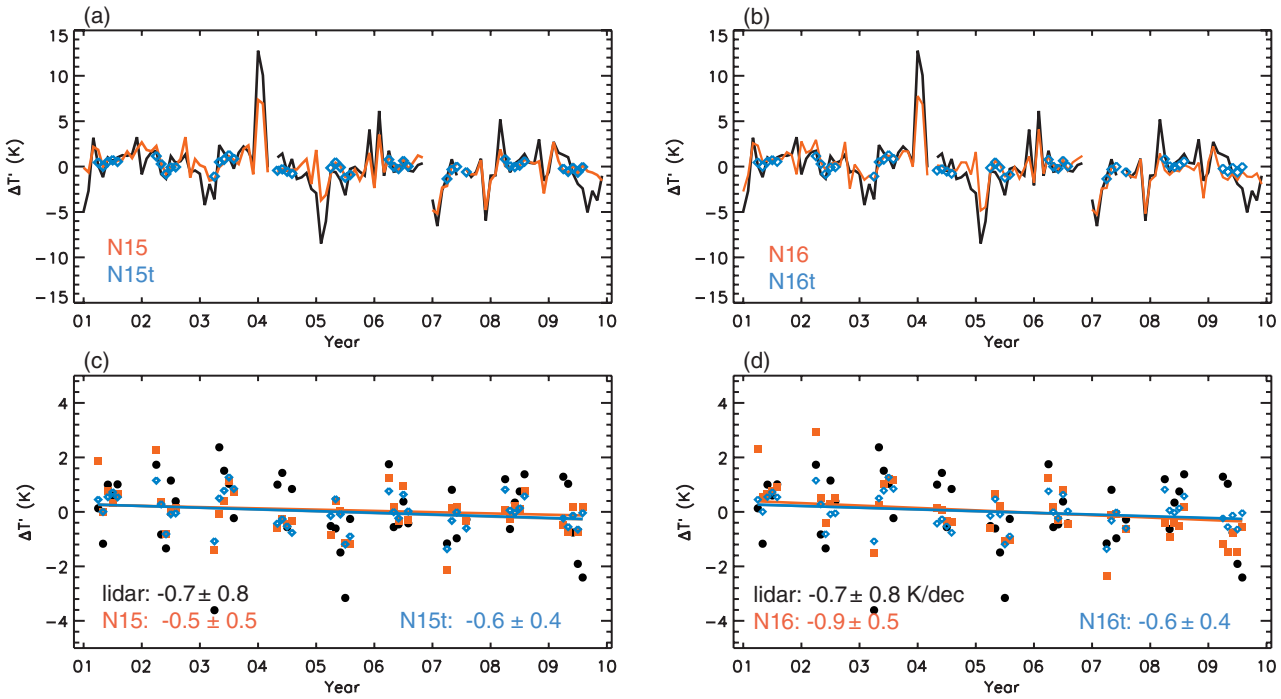

Figure 7. (a)–(d) Time series of temperature anomalies relative to annual cycle for raw AMSU channel 13 temperature before (N15, N16) and after (N15t, N16t) tidal corrections. AMSU time series are compared with Table Mountain Lidar (NDACC-JPL). Linear regressions for lidar and AMSU summer months temperature are compared, including AMSU tidal corrections.

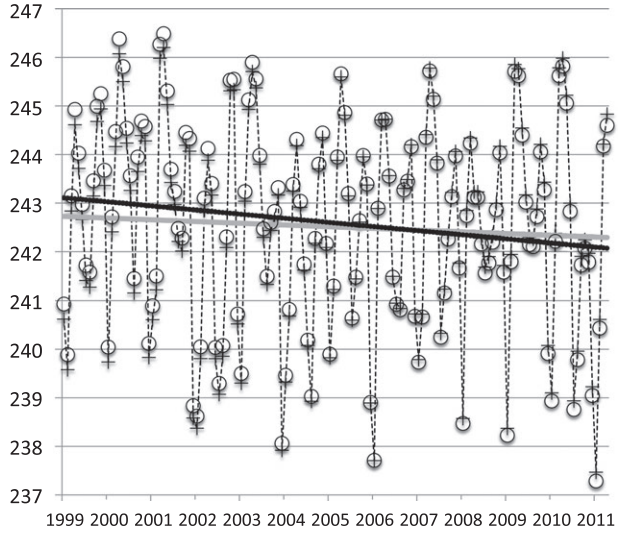

Figure 8. Equatorial raw (plus signs) and tidal-corrected (circles) NOAA-15 adjusted AMSU channel 13 temperature (K) time series and respective derived trend estimates of −0.35 and −0.85 K decade^{-1}.

It is not easy to disentangle the contributions of atmospheric tides from the instrument drift to explain observed temperature drifts between two simultaneous instruments in space on different orbits.

In this study, in assuming that atmospheric tides are the main reason for observed temperature drift between measurements by AMSU on NOAA 15 and 16, diurnal tides are derived for summer months. These compare well with simulated tides, showing that most of the observed temperature drifts may be due to tides. The impact on temperature trend estimates is large and the observed trend induced by tidal effects is of the same order. Such a correction was possible for summer data when the diurnal mode dominates. An extension to other months will require deriving both diurnal and semi-diurnal components. With only two measurement series, an unequivocal tidal solution cannot be derived accurately. However, based on the good agreement found here between models and AMSU observations, we conclude that tidal model estimates can probably be used instead, with a small rescaling.

These corrections on successive instruments over several decades also presuppose that atmospheric tides are stable with time. Such a methodology is limited by two factors. First, atmospheric tides due to ozone and water vapour can have their own variability and potential trends due to climate change and emission of ozone-depleting substances. Second, tides are waves that propagate vertically and depend on temperature and wind fields that also exhibit a large variability and long-term trends. Characteristics of atmospheric tides in such a variable atmosphere are still not well known. However, a sensitivity study shows that long-term changes of tide amplitudes due to expected atmospheric changes remain smaller than 10% (Morel *et al.*, 2004). Only non-migrating tides are considered in this study; however, migrating tide should also contribute, mainly if data are investigated over longitudes.

In most cases, the temperature monitoring is ensured by a succession of instruments, due to their operational status for weather forecasting and temperature monitoring (identified as sentinel instruments), using overlap periods. AMSUs on NOAA 15 and 16 exhibit an unexpectedly long lifetime. However while the instruments are similar, if their times of measurement are different some bias due to tides is superimposed on instrumental bias, as was demonstrated by using AMSU IMICA data (which eliminated most instrument and scene biases). On some platforms, like Metop, the orbit is maintained. However, tidal corrections are still required to separate both effects. If overlap periods do not exist, adjustment and time continuity could be ensured with a ground-based lidar network (Keckhut *et al.*, 2011), and tide corrections should also be considered (Keckhut *et al.*, 1996).

Acknowledgements

This work was performed in the frame of the FP7 ARISE project. This tide issue was discussed during the Stratospheric Temperature Trend Assessment group of the SPARC/WCRP programme and the ISSI (International Space Science Institute) working group ‘Characterizing the diurnal variation of ozone’. AMSU data were provided by the INSU-CNES ICARE thematic

centre (http://www.icare.univ-lille1.fr) with the assistance of the IPSL expert centre ESPRI. NDACC data used in this work are created by NASA-JPL and are archived in the NOAA database at http://www.ndsc.ncep.noaa.gov/. The AMSU IMICA and limb-corrected operational AMSU data used in this study were acquired from NOAA's National Climatic Data Center (http://www.ncdc.noaa.gov). AMSU IMICA was originally developed by Cheng Zhi Zou and colleagues at NOAA though support from NOAA's CDR Program. The authors thank Thierry Leblanc (JPL) and Maura Hagan (HAO) for the suggestions and data. We thank Adrian J. Simmons and an anonymous reviewer for their constructive and positive criticism.

References

Angot G, Keckhut P, Hauchecorne A, Claud C. 2012. Contribution of stratospheric warmings to temperature trends in the middle atmosphere from the lidar series obtained at Haute-Provence Observatory (44°N). *J. Geophys. Res.* **117**: D21102, doi: 10.1029/2012JD017631.

Austin J, Wilson RJ, Akiyoshi H, Bekki S, Butchart N, Claud C, Fomichev VI, Forster P, Garcia RR, Gillett NP, Keckhut P, Langematz U, Manzini E, Nagashima T, Randel WJ, Rozanov E, Shibata K, Shine KP, Struthers H, Thompson DWJ, Wu F, Yoden S. 2009. Coupled chemistry climate model simulations of stratospheric temperatures and their trends for the recent past. *Geophys. Res. Lett.* **36**: L13809, doi: 10.1029/2009GL038462.

Cao C, Weinreb M, Xu H. 2004. Predicting simultaneous nadir overpasses among polar-orbiting meteorological satellites for the intersatellite calibration of radiometers. *J. Atmos. Oceanic Technol.* **21**: 537–542, doi: 10.1175/1520-0426(2004)021<0537:PSNOAP>2.0.CO;2.

David C, Haefele A, Keckhut P, Marchand M, Jumelet J, Leblanc T, Cenac C, Laqui C, Porteneuve J, Haeffelin M, Courcoux Y, Snels M, Viterbini M, Quatrevalet M. 2012. Evaluation of stratospheric ozone, temperature, and aerosol profiles from the LOANA lidar in Antarctica. *Polar Sci.* **6**: 209–225, doi: 10.1016/j.polar.2012.07.001.

Funatsu BM, Claud C, Keckhut P, Hauchecorne A. 2008. Cross-validation of AMSU and lidar for long-term upper-stratospheric temperature monitoring. *J. Geophys. Res.* **113**: D23108, doi: 10.1029/2008JD010743.

Goldberg MD, Crosby DS, Whou L. 2001. The limb adjustment of AMSU-A observations: Methodology and validation. *J. Appl. Meteorol.* **40**: 70–83.

Hagan ME, Burrage MD, Forbes JM, Hackney J, Randel WJ, Zhang X. 1999. GSWM-98: Results for migrating solar tides. *J. Geophys. Res.* **104**: 6813–6827, doi: 10.1029/1998JA900125.

Intergovernmental Panel on Climate Change. 2007. Climate change 2007: The physical science basis. In *Contribution of Working Group I to the Fourth Assessment Report of the Intergovernmental Panel on Climate Change*, Solomon S, Qin D, Manning M, Chen Z, Marquis M, Averyt KB, Tignor M, Miller HL. (eds.): 996 pp. Cambridge University Press: Cambridge, UK and New York, NY.

Karbou F, Aires F, Prigent C, Eymard L. 2005. Potential of Advanced Microwave Sounding Unit-A (AMSU-A) and AMSU-B measurements for atmospheric temperature and humidity profiling over land. *J. Geophys. Res.* **110**: D07109, doi: 10.1029/2004JD005318.

Keckhut P, Gelman ME, Wild JD, Tissot F, Miller AJ, Hauchecorne A, Chanin M-L, Fishbein EJ, Gille J, Russell JM III, Taylor FW. 1996. Semidiurnal and diurnal temperature tides (30–55 km): Climatology and effect on UARS–lidar data comparisons. *J. Geophys. Res.* (special issue on UARS Data Validation) **101**: 10299–10310, doi: 10.1029/96JD00344.

Keckhut P, McDermid S, Swart D, McGee T, Godin-Beekmann S, Adriani A, Barnes J, Baray J-L, Bencherif H, Claude H, Fiocco G, Hansen G, Hauchecorne A, Leblanc T, Lee CH, Pal S, Megie G, Nakane H, Neuber R, Steinbrecht W. 2004. Review of ozone and temperature lidar validations performed within the framework of the network for the detection of stratospheric change. *J. Environ. Monitor.* **6**: 721–733.

Keckhut P, Randel WJ, Claud C, Leblanc T, Steinbrecht W, Bencherif H, McDermid IS, Hauchecorne A, Long C, Lin R, Baumgarten G. 2011. An evaluation of uncertainties in monitoring middle atmosphere temperatures with the lidar network in support of space observation. *J. Atmos. Solar-Terr. Phys.* **73**: 627–642, doi: 10.1016/j.jastp.2011.01.003.

Leblanc T, McDermid IS, Hauchecorne A, Keckhut P. 1998. Evaluation of optimization of lidar temperature analysis algorithms using simulated data. *J. Geophys. Res.* **103**: 6177–6187, doi: 10.1029/97JD03494.

Mears CA, Schabel MC, Wentz FJ. 2003. A reanalysis of the MSU channel 2 tropospheric temperature record. *J. Clim.* **16**: 3650–3664, doi: 10.1175/1520-0442(2003)016<3650:AROTMC>2.0.CO;2.

Morel B, Keckhut P, Bencherif H, Hauchecorne A, Mégie G, Baldy S. 2004. Investigation of the tidal variations in a 3-D dynamics–chemistry–transport model of the middle atmosphere. *J. Atmos. Solar-Terr. Phys.* **66**: 251–265, doi: 10.1016/j.jastp.2003.11.004.

Nash J. 1988. Extension of explicit radiance observations by the Stratospheric Sounding Unit into the lower stratosphere and lower mesosphere. *Q. J. R. Meteorol. Soc.* **114**: 1153–1171.

Nash J, Brownscombe JL. 1982. Validation of the stratospheric sounding unit. *Adv. Space Res.* **2**: 59–62.

Nash J, Edge PR. 1989. Temperature changes in the stratosphere and lower mesosphere 1979–1988 inferred from TOVS radiance observations. *Adv. Space Res.* **9**: 333–341.

Nash J, Forrester GF. 1986. Long-term monitoring of stratospheric temperature trends using radiance measurements obtained by the TIROS-N series of NOAA spacecraft. *Adv. Space Res.* **6**: 37–44.

Powell AM Jr, Xu J, Zou C-Z, Zhao L. 2013. Stratospheric and tropospheric SS/MSU temperature trends and compared to reanalyses and IPCC CMIP 5 simulations in 1979–2005. *Atmos. Chem. Phys. Discuss.* **13**: 3957–3992, doi: 10.5194/acpd-13-3957-2013.

Randel WJ, Shine KP, Austin J, Barnett J, Claud C, Gillett NP, Keckhut P, Langematz U, Lin R, Long C, Mears C, Miller A, Nash J, Seidel DJ, Thompson DWJ, Wu F, Yoden S. 2009. An update of observed stratospheric temperature trends. *J. Geophys. Res.* **114**: D02107, doi: 10.1029/2008JD010421.

Shine KP, Bourqui MS, Forster PMde F, Hare SHE, Langematz U, Braesicke P, Grewe V, Ponater M, Schnadt C, Smith CA, Haigh JD, Austin J, Butchart N, Shindell DT, Randel WJ, Nagashima T, Portmann RW, Solomon S, Seidel DJ, Lanzante J, Klein S, Ramaswamy V, Schwarzkopf MD. 2003. A comparison of model-simulated trends in stratospheric temperatures. *Q. J. R. Meteorol. Soc.* **129**: 1565–1588, doi: 10.1256/qj.02.186.

Shine KP, Barnett JJ, Randel WJ. 2008. Temperature trends derived from stratospheric sounding unit radiances: The effect of increasing CO_2 on the weighting function. *Geophys. Res. Lett.* **35**: L02710, doi: 10.1029/2007GL032019.

Simmons AJ, Poli P, Dee DP, Berrisford P, Hersbach H, Kobayashi S, Peubey C. 2014. Estimating low-frequency variability and trends in atmospheric temperature using ERA-Interim. *Q. J. R. Meteorol. Soc.* **140**: 329–353, doi: 10.1002/qj.2317.

Solomon S, Rosenlof K, Portmann R, Daniel J, Davis S, Sanford T, Plattne G-K. 2010. Contributions of stratospheric water vapour to decadal changes in the rate of global warming. *Science* **327**: 1219–1223, doi: 10.1126/science.1182488.

Thompson DWJ, Seidel DJ, Randel WJ, Zou C-Z, Butler AH, Mears C, Osso A, Long C, Lin R. 2012. The mystery of recent stratospheric temperature trends. *Nature* **491**: 692–697, doi: 10.1038/nature11579.

Wang LK, Zou C-Z. 2013. Intercomparison of SSU temperature data records with Lidar, GPS RO, and MLS observations. *J. Geophys. Res. Atmos.* **118**: 1747–1759, doi: 10.1002/jgrd.50162.

Wang W, Zou C-Z. 2014. AMSU-A only atmospheric temperature data records from the lower troposphere to the top of stratosphere. *J. Atmos. Oceanic Technol.* **31**: 808–825, doi: 10.1175/JTECH-D-13-00134.1.

Wang LK, Zou C-Z, Qian HF. 2012. Construction of stratospheric temperature data records from stratospheric sounding units. *J. Clim.* **25**: 2931–2946, doi: 10.1175/JCLI-D-11-00350.1.

World Meteorological Organization. 2007. 'Scientific assessment of ozone depletion'. Global Ozone Research and Monitoring Project, Report 50. World Meteorological Organization: Geneva, Switzerland.

Wylie DP, Jackson DL, Menzel WP, Bates JJ. 2005. Trends in global cloud cover in two decades of HIRS observations. *J. Clim.* **18**: 3021–3031.

Zhang XL, Forbes JM, Hagan ME. 2010. Longitudinal variation of tides in the MLT region: 1. Tides driven by tropospheric net radiative heating. *J. Geophys. Res.* **115**: A06316, doi: 10.1029/2009JA014897.

Zou C-Z, Wang WH. 2011. Intersatellite calibration of AMSU-A observations for weather and climate applications. *J. Geophys. Res.* **116**: D23113, doi: 10.1029/2011JD016205.